

Removal of Crystal Violet Dye from Aqueous Solution Using Immobilized Spent Coffee Powder

Jia-Jun Teoh¹, Siew-Teng Ong^{1,2*}, and Sie-Tiong Ha^{1,2}

¹Faculty of Science, Universiti Tunku Abdul Rahman, Jl. Universiti, Bandar Barat, 31900 Kampar, Perak, Malaysia

²Center for Agriculture and Food Research, Universiti Tunku Abdul Rahman, Jl. Universiti, Bandar Barat, 31900 Kampar, Perak, Malaysia

* **Corresponding author:**

email: ongst@utar.edu.my

Received: November 7, 2024

Accepted: December 30, 2024

DOI: 10.22146/ijc.101370

Abstract: In this work, the possibility of using immobilized spent coffee powder (ISCP) as an adsorbent for crystal violet (CV) adsorption from an aqueous solution was analyzed. The effect of process parameters such as pH, contact time, number of ISCP films, and initial CV concentrations on the removal of CV was studied. The optimum pH for the adsorption of CV was found to be at pH 7. The adsorption was rapid at the initial stage, and equilibrium was achieved in 100 min. The adsorption of CV increased with the increasing number of ISCP films. Characterization of ISCP was carried out by using FESEM and ATR-FTIR. Langmuir isotherm model can be used to explain the equilibrium data, and a maximum sorption capacity of 97.09 mg/g with a high coefficient of determination (R^2) of 0.9986, was obtained. The experimental data were found to be fitted well into the pseudo-second-order kinetic model. From the Plackett-Burman results, both contact time and pH were identified as significant factors. Under the optimum experimental conditions based on RSM, the percentage uptake predicted by the model was in close agreement with the experimental values.

Keywords: crystal violet; coffee powder; adsorption; kinetics; isotherm

■ INTRODUCTION

Dyes are substances used to add color to various materials such as textiles, fabrics, and leather. These colored substances are chemically bonded to the material they are applied to. Coloring is sometimes considered an essential aspect of the material's development and critical to the end-product appearance. Synthetic dyes for fabric coloring have evolved into a multibillion-dollar industry. While the colored materials look attractive, their waste is toxic to the environment. Dyes harm water bodies and often end up in rivers, lakes, and other water sources, leading to water pollution.

Crystal violet (CV) is a type of triphenylmethane dye commonly used in human and veterinary medicine as a biological stain. It is also used in textile processing industries to dye textiles and to provide a deep violet color to paint and printing ink. CV is also used as a bacteriostatic agent in medical solutions and as an antimicrobial agent to prevent fungal growth in poultry feed. Despite its many

uses, CV is a recalcitrant dye molecule that persists in the environment for a long time and can have toxic effects. It acts as a mitotic poison and a potent carcinogen and promotes tumor growth in some fish species. As a result, CV is considered a biohazard substance [1]. Besides, the undue accumulation of this dye in the human body can also cause serious health issues such as respiratory failures, eye irritation, damage to the eye, paralysis, and kidney illness [2-3].

There are various techniques available to remove dyes from water. These include oxidation or ozonation, membrane separation, photo-degradation, chemical coagulation, flocculation, and adsorption. Among these, chemical coagulation is a fast process that involves precipitating particles by destabilizing colloidal particles. This process is usually followed by filtration, sedimentation, and flocculation. Biological methods such as enzymatic, anaerobic, and aerobic biological treatments are low-cost but less efficient because they take

a long time to break down the dyes [4].

Coffee is one of the world's most consumed beverages and the second-largest traded commodity after petroleum. According to the International Coffee Organization (ICO) report in 2023–2024, a total of 178.0 million 60-kg bags of coffee were produced globally [5]. The rapid growth of cafes in Malaysia has somehow caused the creation and disposal of spent coffee powders without further usage. Although it is possible to use spent coffee powder to produce biodiesel, bio-oil, and biochar [6-7], its practicability usage in other aspects should not be neglected. Coffee mainly comprises cellulose, hemicellulose, caffeine, lignin, pectin, tannin, and polyphenol. Spent coffee powder (SCP) contains a tannin-embedding material with polyphenol groups, onto which dyes can be effectively adsorbed by complexation [8].

The current work focuses on immobilizing SCP (ISCP) onto chitosan thin films as this would overcome the problem associated with separating adsorbent at the end of treatment. Immobilizing fine coffee bean powder onto chitosan thin films can avoid the post-filtration or centrifugation steps, which can be costly in large-scale operations. A preliminary test revealed that native chitosan film showed no uptake towards CV, but with ISCP, a high uptake can be obtained. Chitosan-coffee composites were previously reported for the removal of methylene blue dye [9-10], Pb(II) [11], and pharmaceutical pollutants [12]. Herein, this article reports the CV removal using chitosan-coffee composite, which has not been reported before.

■ EXPERIMENTAL SECTION

Materials

SCP was collected and obtained from a local cafe. Chitosan powder was purchased from Nacalai Tesque Inc. (Japan). CV dye ($C_{25}H_{30}N_3Cl$, 407.979 g/mol) was manufactured and purchased from Bio Basic Canada Inc. and used without any modification or purification. Unless otherwise stated, all chemicals used in this study were of analytical reagent grade.

Instrumentation

Field emission scanning electron microscopy (FESEM, JEOL-JSM-6701F) was used in the project with

an emission current of 4.0 kV and a working distance of 5.8 mm. The surface morphology of ISCP film was analyzed before and after the adsorption of CV dye. Attenuated total reflectance-Fourier transform infrared (ATR-FTIR) spectrometer (Perkin Elmer FTIR Spectrum Two) were used to identify the presence of functional groups in SCP, chitosan, and ISCP films (before and after undergoing adsorption of CV dye). The wavenumber was set from 4000 to 400 cm^{-1} in this analysis.

Procedure

Preparation of ISCP film

The collected SCP was washed and boiled with distilled water to remove the brown color and the residual organics. The cleaned and washed SCP was dried in the oven at 60 °C overnight and then stored in a glass bottle. A 1.00 g chitosan powder (small flake chitosan from crab shell) was dissolved in 2% (v/v) 50 mL of acetic acid solution and stirred until a clear homogenous mixture was obtained. The mixture was stirred thoroughly with 10 mL of glycerol solution (10%, v/v) and 1.00 g of SCP. The mixture was then poured into a mold (10 × 10 cm) for casting and subjected to drying at 60 °C in the oven for 12 h. The film will be detached from the mold and soaked in 0.10 M NaOH solution for 90 s for neutralization. This film was then rinsed thoroughly with distilled water and again subjected to be dried overnight at 60 °C in the oven. This is labeled ISCP and will be sealed in a zip bag for further use.

Preparation of adsorbate

A CV dye stock solution of 1000 mg/L dye was prepared and diluted to achieve the required concentration. To prevent degradation of the CV dye, the prepared stock solution was kept in the dark.

Batch experiments

The initial concentrations of CV, contact time, number of ISCP films and pH of CV solution were varied in the batch studies. For each adsorption experiment, 1000 mL of 30 mg/L CV solution and 3 pieces of ISCP films were placed in a glass tank for 3 h unless otherwise stated. Agitation effect was provided by using an air pump. At a predetermined time intervals, a known volume of dye solution will be withdrawn and its dye concentration

will be determined by using Shimadzu UV-Vis-1700 Double Beam Spectrophotometer. The Eq. (1) was used to calculate the percentage uptake of CV solutions;

$$\% \text{uptake} = \frac{C_0 - C_t}{C_0} \times 100\% \quad (1)$$

where C_0 is the initial concentration of CV (mg/L) and C_t is the concentration of CV at time t (mg/L). The removal efficiency of ISCP towards CV dye was investigated in the pH range of 2–11. The pH of the CV dye solution was adjusted to the required pH value by adding HCl or NaOH solution prior to the experiment. As for the initial dye concentration and contact time, three different concentrations (10, 20, 30 mg/L) were studied, and their dye concentrations at 1, 2, 5, 10, 30, 60, 90, 120, 150, 180, 240, 300, and 360 min were analyzed. Different ISCP films (1, 2, 3 and 4 pieces) were used to identify the optimum number of films for the adsorption process. As in the isotherm study, five different concentrations of CV dye solution (20, 30, 40, 60, and 100 mg/L) were prepared for this analysis.

Optimization study

The factors studied in the batch study were transferred to the Plackett-Burman (PB) design study to identify the significant factors. The resultant factors in the Plackett-Burman design study were continued with the central composite design (CCD) model by response surface methodology (RSM) utilizing Design Expert 7.1.3 software.

RESULTS AND DISCUSSION

Characterization of Adsorbent

The surface morphology of ISCP before and after the CV adsorption was examined using FESEM. The

results from our previous findings showed that native chitosan thin film showed a smooth surface. However, with the introduction of spent coffee bean powder, the adsorbent's surface becomes rough and shows high irregularities. The SEM image of ISCP before adsorption (Fig. 1(a)) demonstrated irregularities and lack of pores and cavities. As for the SEM image after the adsorption process (Fig. 1(b)), it is evident that some of the clustering effect was observed due to the CV adsorption. In another work involving commercial coffee wastes as adsorbent, the rough and high irregularities surface of the adsorbent can enhance the adsorption process [13]. After the CV adsorption, a smoother surface of ISCP was observed, which can be related to the coverage of the CV molecules. Similar findings were observed in the previous works [14–17]. The presence of major elements such as C and O in both chitosan and ISCP were confirmed by the EDX analysis. The elemental values of carbon and oxygen in native chitosan films were 55.43 and 44.57%, respectively. However, with the incorporation of spent coffee bean powder, a high carbon content material, the elemental value of C was increased to 60.44% in ISCP.

Fig. S1 shows the FTIR spectra of SCP, chitosan, and ISCP before and after the adsorption of CV dye. As observed in Fig. S1(a), the SCP FTIR spectrum consists of bands characteristic of lignocellulosic materials because its major components are hemicellulose, cellulose, lignin, and other small molecules [18]. The broadband centered at 3350 cm^{-1} is related to the O–H stretching, and the bands at 2920 and 2852 cm^{-1} are related to the aliphatic C–H stretching vibration. The band

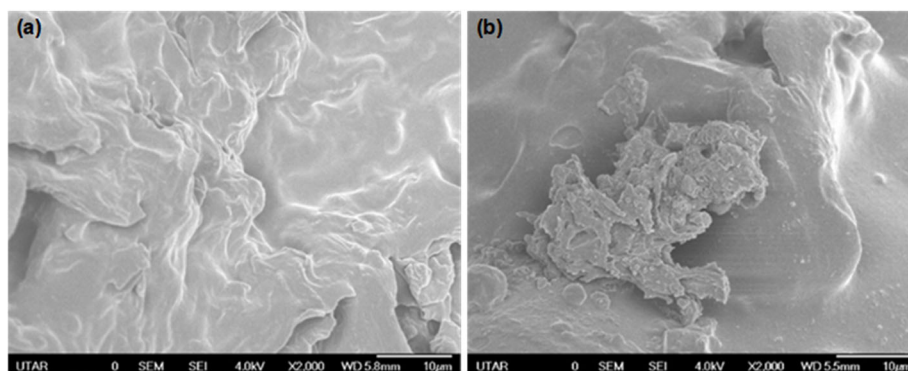


Fig 1. FESEM morphology of ISCP (a) before and (b) after the adsorption of CV

at 1743 cm^{-1} is associated with the C=O stretching of hemicellulose [12]. The FTIR spectrum of chitosan showed stretching vibrations of O–H, N–H, C–H, and C=O (amide I). Since both chitosan and SCP are biomass materials, they showed a similar broad band between 1100 and 900 cm^{-1} due to C–C, C–O–C, and C–O–H bonds [19–21].

Immobilization of SCP onto chitosan film was successful based on the FTIR spectrum (Fig. S1(b)) whereby C=O stretching of hemicellulose (from SCP) and C=O amide I from chitosan absorption bands can be seen at 1743 and 1649 cm^{-1} , respectively. Comparison between chitosan and ISCP (Fig. S1(b)) obviously showed that the weak C–H aliphatic absorption band of chitosan becomes more intense in the ISCP spectrum after SCP was immobilized onto chitosan proposed that chemical crosslinking of chitosan and SCP. The appearance of the absorption band at 1743 cm^{-1} at the ISCP spectrum but not in the chitosan spectrum also indicates that SCP was immobilized onto chitosan.

Table 1 presents the FTIR data of ISCP before and after the adsorption of CV dye. After adsorption of CV onto the ISCP, it was observed that the intensity of the absorption band at 1742 cm^{-1} is significantly reduced (Fig. S1(c)). This band is due to the C=O stretching. It suggests that the CO_2^- group is involved in the binding with the cationic CV dye, which carries the positive charge. Another evidence suggests the successful binding of CV dye onto the ISCP film is the band due to the C–N stretching of aromatic tertiary amine of CV, which can be observed at 1369 cm^{-1} in the ISCP spectrum after adsorption (Fig. S1(c)). This value is close with the value reported for CV dye [22].

Effect of pH

The efficiency of an adsorption process can be strongly affected by the effect of pH since this factor can

affect the degree of ionization of the adsorbate and the surface properties of the adsorbent. The point of zero charge (pH_{pzc}) was determined to be 7.5, which is similar to the results reported by Sertoli et al. [23]. Therefore, the ISCP's surface will carry a net zero charge at its pH_{pzc} . The surface of the adsorbent is positively charged at pH below 7.5 and negatively charged at pH above 7.5. Based on Fig. 2, the lowest amount of CV dye adsorbed by ISCP was at pH 2, which was 58.41%. Thereafter, an increase in the percentage uptake of CV was detected when the pH of the solution was increased. From pH 6–10, an appreciable amount of CV can be removed. The simultaneous occurrence of different kinds of interactions such as electrostatic attraction, hydrogen bonding and π - π interaction, can contribute to this kind of optimum uptake over a pH range. The maximum adsorption of 98.13% of CV was recorded at pH 7. A further increase in dye uptake between pH 8 and 11 was insignificant. The insignificant dye uptake might indicate a cationic exchange process between the dye molecule and the ISCP with the release of hydrogen ions (H^+). Another CV adsorption study has also reported similar behavior [24].

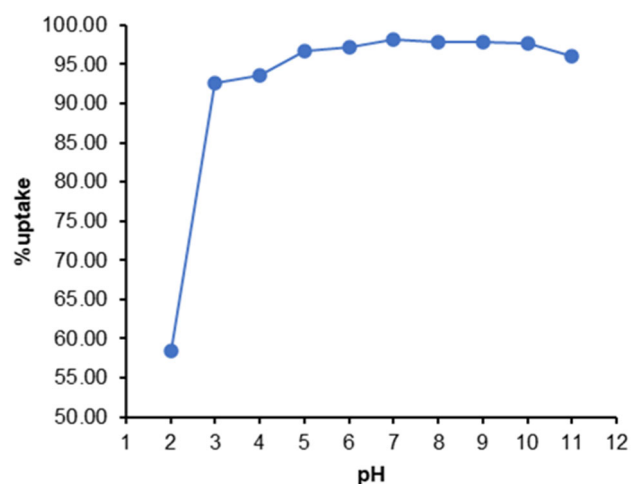


Fig 2. Effect of pH on the adsorption of CV onto ISCP

Table 1. Assignment of peaks for ISCP before and after the adsorption of CV

Functional group	Wavenumber (cm^{-1})	
	ISCP before adsorption	ISCP after adsorption
O–H stretching	3290	3292
C–H stretching	2923, 2855	2924, 2855
C=O stretching	1743	1742
C–N stretching (CV dye)	-	1369

A lower uptake under acidic conditions is because the $-\text{CO}_2\text{H}$ group of ISCP could hardly dissociate in water to form CO_2^- ions as there was a high level of hydronium ions (H_3O^+) present. The positively charged CV (protonated in acidic condition) competed with the H_3O^+ for the vacant sites on the ISCP. The competition between the H_3O^+ and adsorbate caused the low percentage uptake in acidic conditions. When the pH increased, the concentration of H_3O^+ decreased while hydroxide ions (OH^-) increased. CV dye became deprotonated in basic conditions and formed an anion, which would compete with the OH^- in the solution [25].

Effect of Initial Concentration and Contact Time

Based on the results of the experiment, it was observed that as the time interaction between the ISCP and CV increased, the percentage uptake of CV also increased. There was a rapid adsorption in the first 40 min, but it gradually became slower. The equilibrium was established after 90 min. Thus, a contact time of 3 h with dye solutions was used in all the subsequent parameters studied (Fig. 3).

The dye uptake rate and adsorption capacity are higher in the beginning due to the large surface area of the adsorbents available for the adsorption of the CV. However, after a certain amount of time, the remaining vacant sites become less and more difficult to occupy due to repulsive forces between the CV molecules on the solid and bulk phase of ISCP and due to the intraparticle diffusion effect [26].

Sorption Kinetics

The experimental data from the effect of contact time was fitted into different equations to provide more insight into the kinetics involved in the CV dye adsorption by ISCP. Both pseudo-first and pseudo-second-order-model equations were used. The one with a higher value of the linear coefficient of determination (R^2) will be chosen to explain the kinetics involved in the adsorption process. The assumption that proposed by Lagergren [27] is that the change in surface adsorption site concentration over time is proportional to the remaining amount of unoccupied adsorption site [28]. The linear logarithm equation of the pseudo-first-order-model was shown in Eq. (2);

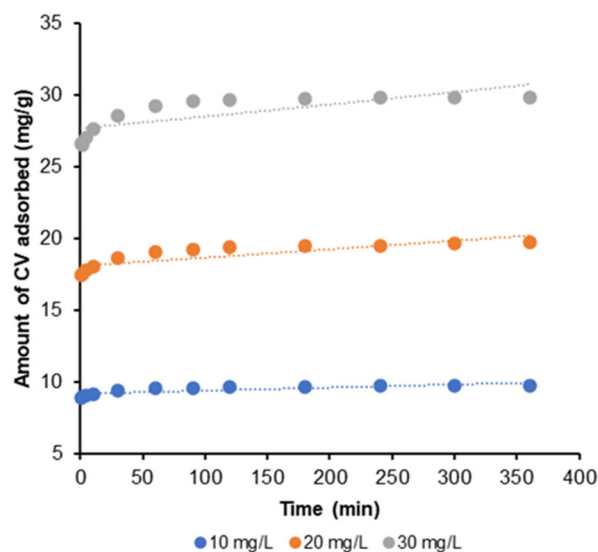


Fig 3. Effect of contact time and initial concentration on the amount of CV adsorbed onto ISCP

$$\log(q_e - q_t) = \log q_e - \frac{k_1}{2.303} t \quad (2)$$

where q_t and q_e are the amount of adsorbate adsorbed at time t and equilibrium (mg/g), respectively. Then, k_1 is the rate constant of pseudo-first-order kinetics (min^{-1}) and t is the adsorption time (min).

The relatively low R^2 values, 0.0266, 0.1314, and 0.1320 were obtained (Table 2). The low R^2 values indicated that the pseudo-first-order model could not adequately explain the adsorption process. According to the results obtained, there was a significant difference between the theoretical and experimental q_e values.

The pseudo-second-order kinetics model stated that the rate of reaction is proportional to the square of the remaining amount of the surface adsorption site, and this model was more inclined towards chemisorption. It also stated the rate-determining step in the chemisorption involves the electrostatic valence forces existing between the adsorbate and adsorbent [29]. The equation of the pseudo-second-order kinetics model was presented in Eq. (3) and (4);

$$\frac{t}{q_t} = \frac{1}{h} + \frac{1}{q_e} \quad (3)$$

$$h = k_2 q_e^2 \quad (4)$$

where h is the initial adsorption rate ($\text{mg g}^{-1} \text{min}^{-1}$) and k_2 is the rate constant of pseudo-second-order kinetics ($\text{g g}^{-1} \text{min}^{-1}$).

Table 2. Kinetic models parameters, theoretical and experimental q_e , and R^2 of pseudo-first and pseudo-second-order kinetics

Initial CV concentration (mg/L)	Pseudo-first-order				
	q_e cal (mg/g)	q_e exp (mg/g)	k_1 (min^{-1})	R^2	
10	0.3955	9.7920	0.0048	0.0266	
20	1.1885	19.7120	0.0062	0.1314	
30	1.3059	29.8310	0.0058	0.1320	
Initial CV concentration (mg/L)	Pseudo-second-order				
	q_e cal (mg/g)	q_e exp (mg/g)	k_2 (g/mg min)	h (mg/g min)	R^2
10	9.7847	9.7920	10.6952	0.1115	1.0000
20	19.6850	19.7120	16.0000	0.0412	0.9999
30	29.8507	29.8310	39.0625	0.0439	1.0000

Based on Table 2, the relatively high R^2 values, which were 0.9999 and unity, were obtained using a pseudo-second-order-kinetics equation. The theoretical and actual values of q_e were relatively close to each other, and it was concluded that this adsorption mechanism fitted the pseudo-second-order kinetics model. Therefore, the pseudo-second-order kinetics model is suggested to be a better representative model to be used in explaining the CV adsorption process onto ISCP compared to the pseudo-first-order. This also implies that the rate limiting step may be chemisorption involving valency forces through the sharing or exchange of electrons between the CV and ISCP. In most adsorption processes involving biosorbent, this model is often considered to be a more appropriate representative kinetic model. In addition, it also offers some advantages, such as not assigning an effective adsorption capacity, the rate constant of pseudo-second-order, and the initial adsorption rate can all be determined from the equation without knowing any parameter beforehand [30-31]. Similar results that reported the applicability of the pseudo-second-order kinetics model have also been observed in the adsorption process involving methylene blue by geopolymer and salacca skin waste [32-33], Congo red by TEPA-PH composite beads [34] and rhodamine B by $\gamma\text{-Fe}_2\text{O}_3/\text{Mt}$ and $\gamma\text{-Fe}_2\text{O}_3$ [35].

Effect of the Number of ISCP films

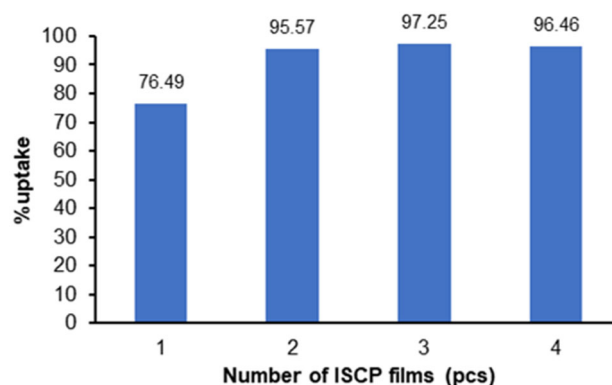
The experimental results revealed that the efficiency of removing CV improved as the amount of adsorbent increased from one to four pieces of ISCP. The maximum

uptake of 97.25% was achieved when three pieces of ISCP were used in the adsorption process, as shown in Fig. 4.

The possible explanation for the higher percentage of dye uptake is the availability of surface-active sites with more active functional groups. However, the overlapping and aggregation of active sites on the ISCP may have led to a slight decrease in the adsorption uptake of CV when the ISCP films were four pieces, as has been observed in the previous work [36].

Isotherm Study

In this study, the Langmuir [37] and Freundlich [38] isotherm models were used to analyze the equilibrium data. The adsorption capacity, type of coverage, and rate constants can be determined using these adsorption isotherm models. The R^2 values were used to determine which model would be more applicable

**Fig 4.** Effect of number of ISCP films on the adsorption of CV onto ISCP

to explain the equilibrium sorption process.

Langmuir states that the adsorption of adsorbate takes place on the homogeneous surface by monolayer adsorption without the interactions of adsorbed ions. Applying the Langmuir isotherm model could identify the maximum adsorption capacity of ISCP. The Langmuir equation is presented in Eq. (5);

$$\frac{C_e}{q_e} = \frac{C_e}{q_m} + \frac{1}{K_L q_m} \quad (5)$$

where q_e is the amount of adsorbate adsorbed at equilibrium (mg/g), q_m is the maximum adsorption capacity of adsorbent (mg/g), K_L is the Langmuir isotherm constant (mg/g), and C_e is the concentration of adsorbate in equilibrium (mg/L).

The relatively high R^2 value of 0.9986 showed that the adsorption process could be explained by Langmuir isotherm (Fig. 5). By using the gradient of the plot and the interception point of y from the graph, the values of q_m and K_L were calculated, which are 97.09 mg/g and 0.7305 L/mg,

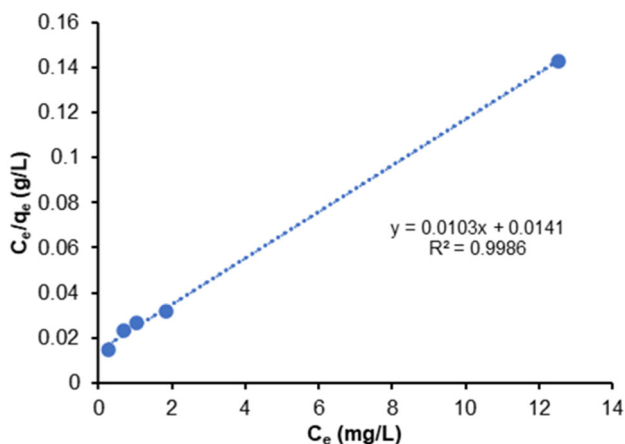


Fig 5. Langmuir isotherm for the adsorption of CV onto ISCP

Table 3. Comparison of maximum adsorption capacity of CV onto different adsorbents

Adsorbent	q_0 (mg/g)	Ref.
Xanthated rice husk	90.02	[25]
Almond shell	12.20	[39]
Peanut husk	20.95	[40]
Lemon wood AC	23.60	[41]
Olive leaves powder	133.33	[42]
Waste fabric polyester	74.80	[43]
ISCP	97.09	This study

respectively. The q_m value of ISCP towards CV is considered high and comparable with other adsorbents previously reported in the literature (Table 3).

The separation factor, R_L , which is a dimensionless constant, is used to describe the essential properties of the Langmuir isotherm. The R_L values obtained from the different adsorbate concentrations were all between 0 and 1, which indicated the adsorption process is favorable. Therefore, the results obtained fitted well in Langmuir isotherm. The Freundlich equation was presented in Eq. (6);

$$\log q_e = \log K_F + \frac{1}{n} \log C_e \quad (6)$$

where n is the Freundlich isotherm constant, and K_F is the Freundlich constant for adsorption capacity (L/mg).

The K_F and n values were 2.22×10^{-4} L/mg and 224.39, respectively. A low R^2 value was obtained from the plot, which was 0.9345, which showed that the adsorption of CV onto ISCP could not be appropriately described by Freundlich isotherm (Fig. 6).

Optimization Study

Plackett-Burman design

The PB design is used to determine the relative importance of different factors that influence the percentage uptake in the adsorption process. It helps identify the significant parameter for further optimization and provides an unbiased estimate of the linearity of all variables with maximum accuracy for a given number of

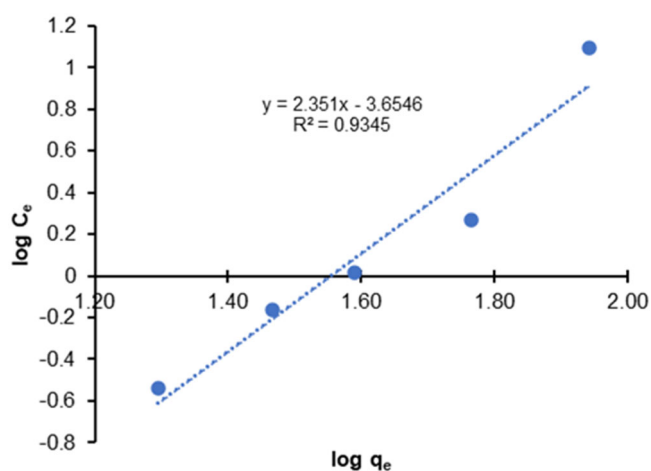


Fig 6. Freundlich isotherm for the adsorption of CV onto ISCP

observations. The reason for choosing PB is that it enables the experimenters to study a large number of factors with a significantly reduced number of experimental runs. The four parameters (pH, initial concentration, contact time, and number of ISCP films) were tested using the PB design model and screened in 11 experimental designs. The experimental results based on PB design and analysis of variance (ANOVA) of PB for the CV removal were tabulated in Tables 4 and 5, respectively. The model term is determined as significant when the p-value is less than 0.05.

Based on the results obtained, the F-value and p-value are 13.10 and 0.0023, respectively, which indicates the model to be significant. Contact time and pH are the most important variables, with low p-values of 0.0288 and 0.0004, respectively. Similar findings have been

previously whereby the uptake of adsorbate molecules is more dependent on contact time and pH [44]. The initial concentration and ISCP films do not significantly affect the response (p-values = 0.1469 and 0.1686, respectively). The R^2 value indicates that the model explains 88.21% of the variance in the response variable, suggesting a good fit. The difference between R^2 and the adjusted R^2 demonstrates that the model is robust without overly complex. The predicted R^2 value of 0.8148 aligns reasonably well with the adjusted R^2 value of 0.6537, as the difference between them is less than 0.2. Any lack of fit is entirely attributed to residual variance, particularly since no significant p-value is reported for the lack of fit term. The function of desirability was applied to validate the model. The experiments were performed under conditions generated by PB and were chosen based on the

Table 4. PB results for the removal of CV by ISCP

Run	Initial concentration (mg/g)	Contact time (min)	pH	ISCP films (pcs)	Experimental %uptake	Predicted %uptake	%difference
1	100	1	2	1	63.24	55.54	-7.70
2	100	1	11	4	75.27	80.69	5.42
3	100	360	2	1	66.92	69.98	3.06
4	100	360	2	4	73.08	63.39	-9.79
5	100	360	11	1	98.20	100	1.80
6	10	1	2	1	38.65	46.95	8.30
7	10	1	2	4	40.35	38.87	-1.48
8	10	1	11	1	90.14	80.18	-9.96
9	10	360	2	4	44.31	53.31	9.00
10	10	360	11	1	93.33	94.62	1.29
11	10	360	11	4	93.72	86.54	-7.18

Table 5. ANOVA of PB for the adsorption of CV by ISCP

Source	Sum of squares	Degree of freedom	Mean square	F-value	p-value
Model	4355.20	4	1088.80	13.10	0.0023
A-Initial concentration	221.10	1	221.10	2.66	0.1469
B-Contact time	625.62	1	625.62	7.53	0.0288
C-pH	3312.59	1	3312.59	39.85	0.0004
D-ISCP films	195.88	1	195.88	2.36	0.1686
Residual	581.84	7	83.12		
Lack of fit	581.84	6	96.97		
Std. Dev.	9.12			R^2	0.8821
				Adjusted R^2	0.8148
				Predicted R^2	0.6537
				Adeq. precision	10.9321

highest desirability. The experimental conditions as well as the predicted and experimental results, were tabulated in Table 4. The percentage difference was all less than 10%.

The results show that pH significantly influences dye removal by affecting both the dye's ionization and the adsorbent surface properties. The dependence of dye uptake on contact time can be attributed to three phases of dye adsorption: (i) external mass transfer or instantaneous adsorption, (ii) gradual adsorption with intra-particle diffusion as a rate-controlling factor, and (iii) final equilibrium where intra-particle diffusion slows down due to low solute concentration in the solution [45].

Response surface methodology approach

The crucial parameters affecting the percentage of dye uptake were further studied using the CCD under the RSM approach. Table 6 shows the comparison of the %uptake between the predicted and experimental results for the effect of pH and contact time of CV dye. A modified quadratic model was used to describe the

correlation between two variables and the percentage uptake, and the final equation in terms of coded factors is shown in Eq. (7);

$$\% \text{uptake} = 18.85374392 + 0.21427891(A) + 12.167873(B) - 0.004472(AB) - 0.00032(A^2) - 0.596929(B^2) \quad (7)$$

where A = contact time and B = pH.

The model was significant, with $p < 0.0001$ and F-value of 52.72. The R^2 , adjusted R^2 , and predicted R^2 were found to be 0.9741, 0.9557, and 0.7889, respectively (Table 7). The R^2 value shows how well the data fit the regression model (the goodness of fit), whereas the adjusted R^2 provides an accurate model that fits the current data. For the predicted R^2 , it determines how well a regression model can make an accurate prediction for future data. The closer the R^2 is to unity, the stronger the model is and the better it is at predicting the response. With an R^2 value close to unity, it is estimated that there will be a close agreement between the experimental and predicted uptake by the model. The

Table 6. RSM results of the removal of CV by ISCP

Run	Contact time (min)	pH	Experimental %uptake	Predicted %uptake	%difference
1	1	2	44.1781	41.008	-3.1701
2	1	6.5	66.1419	72.915	6.7731
3	1	11	84.2497	80.646	-3.6037
4	180.5	2	64.7009	67.452	2.7511
5	180.5	6.5	97.0205	95.746	-1.2745
6	180.5	11	96.2453	99.865	3.6197
7	360	2	72.8801	73.298	0.4179
8	360	6.5	98.3820	97.980	-0.4020

Table 7. ANOVA of RSM for the adsorption of CV by ISCP

Source	Sum of squares	Degree of freedom	Mean square	F-value	p-value
Model	3691.58	5	738.32	52.72	< 0.0001
A-Contact time	942.35	1	942.35	67.29	< 0.0001
B-pH	1575.84	1	1575.84	112.52	< 0.0001
AB	52.20	1	52.20	3.73	0.0948
A ²	292.95	1	292.95	20.92	0.0026
B ²	403.56	1	403.56	28.82	0.0010
Residual	98.03	7	14.00		
Lack of fit	98.03	3	32.68		
Std. Dev.	3.74				
			R ²	0.9741	
			Adjusted R ²	0.9557	
			Predicted R ²	0.7889	
			Adeq. Precision	23.1500	

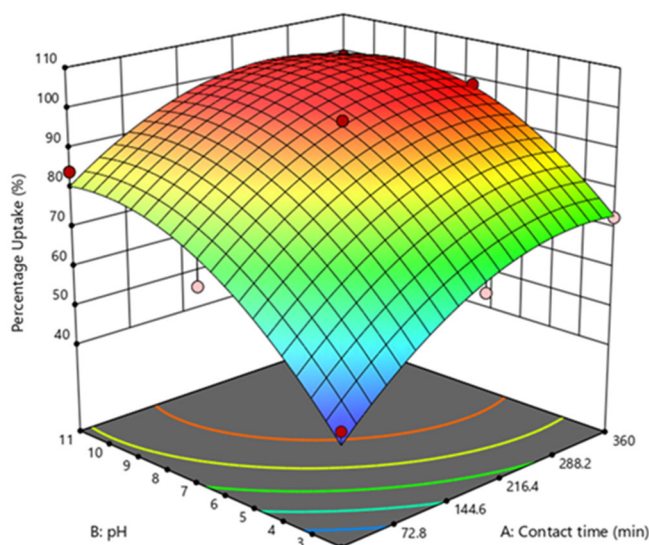


Fig 7. 3D surface plot for percentage uptake of CV by ISCP as a function of contact time and pH at 30 mg/L initial concentration

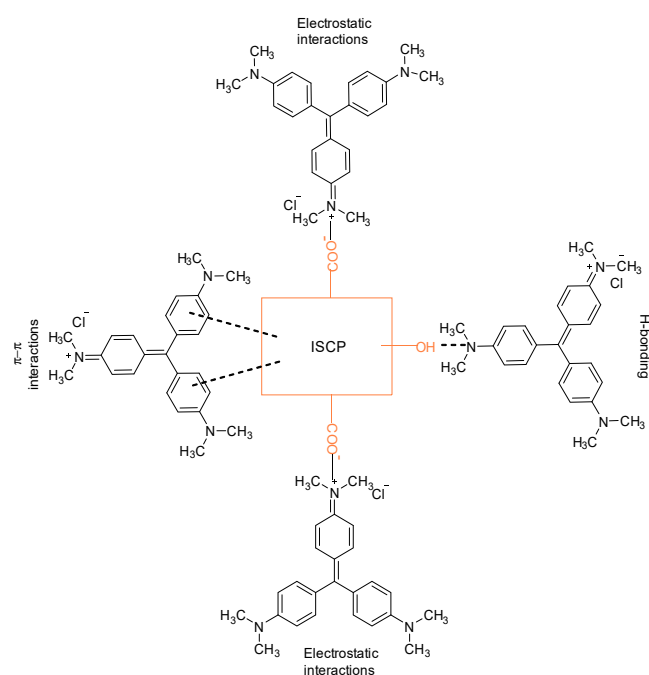


Fig 8. Adsorption mechanism of CV dye on ISCP adsorbent

predicted R^2 value of 0.9557 is in reasonable agreement with the adjusted R^2 value of 0.7889, and the difference is less than 0.2. The coefficient of variance (C.V.) of this model was reported as 4.38%. The lower the C.V. value, the greater is the precision and reliability of the experiments carried out. Adequate precision measures

the signal-to-noise ratio, and a ratio greater than 4 is desirable whereas in this study, the ratio of 23.150 indicates an adequate signal.

Fig. 7 shows the 3D surface plot for the percentage uptake of CV by ISCP as a function of contact time and pH at 30 mg/L initial concentration. The maximum percentage uptake of CV dye was observed when the contact time and pH were at 360 min and 6.5, respectively. At these operational values, the model predicted a 97.98% uptake. A similar observation was reported in the removal of methylene blue dye in the Chan and Ong study [46], whereby the optimum condition was achieved under longer contact time and higher pH.

Adsorption Mechanism

Various interactions took place between adsorbent and adsorbate during the adsorption process. It has been reported that cationic CV dye adsorbed to the surface of adsorbent via interactions such as hydrogen bonding, π - π interactions, and electrostatic attraction [3,47]. The surface of adsorbent has negative functionalities at $\text{pH} > \text{pH}_{\text{zpc}}$, which shows extensive electrostatic interaction with dye molecules and plays a major role in removing CV from the aqueous solution. In most cases, the charge is the driving force of the adsorption process. In the system under consideration, if the surface has a negative charge, electrostatic attraction of CV cations very favorably occurred [47]. The O-H groups present on the surface of ISCP played a role in hydrogen bonding with nitrogen atoms of CV dye. The π electrons of CV molecules were involved in π - π interactions with the ISCP. All these interactions are shown on Fig. 8.

CONCLUSION

Removal of CV dye using ISCP was conducted in this project. The successful binding of CV onto ISCP film was confirmed based on the ATR-FTIR analysis whereby the change in intensity of the C=O stretching band and appearance of C-N stretching of aromatic tertiary amine of CV dye were observed after the adsorption process. Based on the SEM images, a more irregular surface can be observed on the ISCP before the adsorption compared to the one after CV adsorption.

The highest CV removal was found to be at pH 7. Based on the kinetics studies, the CV adsorption process onto the ISCP fitted well into the pseudo-second-order model. The relatively high R^2 value, 0.9986, indicated that the Langmuir isotherm model can be used to explain the experimental results, and the maximum adsorption capacity was calculated to be 97.09 mg/g. PB design identified the contact time and pH as significant factors influencing the CV percentage uptake. By using RSM, a set of optimal experimental conditions for CV uptake was obtained with the compromise of this response: contact time (360 min), initial concentration (30 mg/L), number of ISCP films (3 pcs), and pH (6.5).

■ ACKNOWLEDGMENTS

The authors are thankful for the research facilities provided by Universiti Tunku Abdul Rahman, Malaysia.

■ CONFLICT OF INTEREST

The authors have no conflict of interest to be declared.

■ AUTHOR CONTRIBUTIONS

Jia-Jun Teoh: data curation, formal analysis, investigation, methodology, validation, visualization, writing-original draft, writing-review and editing. Siew-Teng Ong: conceptualization, methodology, funding acquisition, project administration, resources, supervision, validation, writing-review and editing. Sie-Tiong Ha: conceptualization, methodology, funding acquisition, project administration, supervision, validation, writing-review and editing. All authors agreed to the final version of this manuscript.

■ REFERENCES

- [1] Kumar, N., Rosy, R., and Sharma, Y.C., 2025, Biomass derived gamma alumina decorated mesoporous carbon adsorbent for crystal violet removal from aqueous solution using batch system: Isotherm, thermodynamic and kinetic modelling, *J. Mol. Struct.*, 1322 (Part 2), 140365.
- [2] Mulla, B., Ioannou, K., Kotanidis, G., Ioannidis, I., Constantinides, G., Baker, M., Hinder, S., Mitterer, C., Pashalidis, I., Kostoglou, N., and Rebholz, C., 2024, Removal of crystal violet dye from aqueous solutions through adsorption onto activated carbon fabrics, *C*, 10 (1), 19.
- [3] Kumbhar, P., Narale, D., Bhosale, R., Jambhale, C., Kim, J.H., and Kolekar, S., 2022, Synthesis of tea waste/ Fe_3O_4 magnetic composite (TWMC) for efficient adsorption of crystal violet dye: Isotherm, kinetic and thermodynamic studies, *J. Environ. Chem. Eng.*, 10 (3), 107893.
- [4] Al-Tohamy, R., Ali, S.S., Li, F., Okasha, K.M., Mahmoud, Y.A.G., Elsamahy, T., Jiao, H., Fu, Y., and Sun, J., 2022, A critical review on the treatment of dye-containing wastewater: Ecotoxicological and health concerns of textile dyes and possible remediation approaches for environmental safety, *Ecotoxicol. Environ. Saf.*, 231, 113160.
- [5] International Coffee Organization, 2023, Coffee Report and Outlook, *Executive Summary*, International Coffee Organization, London, UK.
- [6] Juliastuti, S.R., Widjaja, T., Altway, A., Sari, V.A., Arista, D., and Iswanto, T., 2018, The effects of microorganism on coffee pulp pretreatment as a source of biogas production, *MATEC Web Conf.*, 156, 03010.
- [7] Atabani, A.E., Ali, I., Naqvi, S.R., Badruddin, I.A., Aslan, M., Mahmoud E., Almomani, F., Juchelková, D., Atelge, M.R., and Yunus Khan, T.M., 2022, A state-of-the-art review on spent coffee ground (SCG) pyrolysis for future biorefinery, *Chemosphere*, 286 (Part 2), 131730.
- [8] Kim, M.S., and Kim, J.G., 2020, Adsorption characteristics of spent coffee grounds as an alternative adsorbent for cadmium in solution, *Environments*, 7 (4), 24.
- [9] Nugraheni, A.D., Nurmayasari, N., and Sholihun, S., 2024, Performance of chitosan beads after treatment with spent coffee grounds for the adsorption of methylene blue, *Coffee Sci.*, 19, e192241.
- [10] Ozudogru, Y., and Tekne, E., 2023, Adsorption of methylene blue from aqueous solution using spent coffee/chitosan composite, *J. Water Chem. Technol.*, 45 (3), 234–245.

- [11] Choi, H.J., 2019, Applicability of composite beads, spent coffee grounds/chitosan, for the adsorptive removal of Pb(II) from aqueous solutions, *Appl. Chem. Eng.*, 30 (5), 536–545.
- [12] Lessa, E.F., Nunes, M.L., and Fajardo, A.R., 2018, Chitosan/waste coffee-grounds composite: An efficient and eco-friendly adsorbent for removal of pharmaceutical contaminants from water, *Carbohydr. Polym.*, 189, 257–266.
- [13] Milanković, V., Tasić, T., Pejčić, M., Pašti, I., and Lazarević-Pašti, T., 2023, Spent coffee grounds as an adsorbent for malathion and chlorpyrifos—Kinetics, thermodynamics, and eco-neurotoxicity, *Foods*, 12 (12), 2397.
- [14] Sukla Baidya, K., and Kumar, U., 2021, Adsorption of brilliant green dye from aqueous solution onto chemically modified areca nut husk, *S. Afr. J. Chem. Eng.*, 35, 33–43.
- [15] Mondal, N.K., and Kar, S., 2018, Potentiality of banana peel for removal of congo red dye from aqueous solution: Isotherm, kinetics and thermodynamics studies, *Appl. Water Sci.*, 8 (6), 157.
- [16] Aljeboree, A.M., and Alkaim, A.F., 2024, Studying removal of anionic dye by prepared highly adsorbent surface hydrogel nanocomposite as an applicable for aqueous solution, *Sci. Rep.*, 14 (1), 9102.
- [17] Chong, J.K., and Ong, S.T., 2021, Utilization of banana peel as a biosorbent for the removal of basic red 29 from aqueous solution, *Stud. Univ. Babeş-Bolyai Chem.*, 66 (4), 171–187.
- [18] Ballesteros, L.F., Teixeira, J.A., and Mussatto, S.I., 2014, Chemical, functional, and structural properties of spent coffee grounds and coffee silverskin, *Food Bioprocess Technol.*, 7 (12), 3493–3503.
- [19] Heredia-Guerrero, J.A., Benítez, J.J., Domínguez, E., Bayer, I.S., Cingolani, R., Athanassiou, A., and Heredia, A., 2014, Infrared and Raman spectroscopic features of plant cuticles: A review, *Front. Plant Sci.*, 5, 305.
- [20] Alves, N.O., da Silva, G.T., Webber, D.M., Luchese, C., Wilhem, E.A., and Fajardo, A.R., 2016, Chitosan/poly(vinyl alcohol)/bovine bone powder biocomposites: A potential biomaterial for the treatment of atopic dermatitis-like skin lesions, *Carbohydr. Polym.*, 148, 115–124.
- [21] Kloster, G.A., Marcovich, N.E., and Mosiewicki, M.A., 2015, Composite films based on chitosan and nanomagnetite, *Eur. Polym. J.*, 66, 386–396.
- [22] Cheriaa, J., Khairiddine, M., Rouabhia, M., and Bakhrouf, A., 2012, Removal of triphenylmethane dyes by bacterial consortium, *Sci. World J.*, 2012 (1), 512454.
- [23] Sertoli, L., Carnier, R., de Abreu, C.A., Coscione, A.R., and Melo, L.C.A., 2019, Coffee waste biochars: Characterization and zinc adsorption from aqueous solution, *Coffee Sci.*, 14 (4), 518–529.
- [24] Lairini, S., El Mahtal, K., Miyah, Y., Tanji, K., Guissi, S., Boumchita, S., and Zerrouq, F., 2017, The adsorption of crystal violet from aqueous solution by using potato peels (*Solanum tuberosum*): Equilibrium and kinetic studies, *J. Mater. Environ. Sci.*, 8 (9), 3252–3261.
- [25] Homagai, P.L., Poudel, R., Poudel, S., and Bhattarai, A., 2022, Adsorption and removal of crystal violet dye from aqueous solution by modified rice husk, *Heliyon*, 8 (4), e09261
- [26] Ashna, P., and Heydari, R., 2020, Removal of reactive red 198 from aqueous solutions using modified clay: Optimization, kinetic and isotherm, *J. Chil. Chem. Soc.*, 65 (4), 4958–4961.
- [27] Lagergren, S., 1898, About the theory of so-called adsorption of soluble substances, *K. Sven. Vetenskapsakad. Handl.*, 24, 1–39.
- [28] Musah, B.I., Peng, L., and Xu, Y., 2020, Adsorption of methylene blue using chemically enhanced *Platanus orientalis* leaf powder: Kinetics and mechanisms, *Nat. Environ. Pollut. Technol.*, 19 (1), 29–40.
- [29] Ho, Y.S., and McKay, G., 1999, Pseudo-second order model for sorption processes, *Process Biochem.*, 34 (5), 451–465.
- [30] Gan, H.Y., Leow, L.E., Ong, S.T., 2017, Utilization of corn cob and TiO₂ photocatalyst thin films for dyes removal, *Acta Chim. Slov.*, 64, 144–158.
- [31] Ho, Y.S., 2006, Review of second-order models for adsorption systems, *J. Hazard. Mater.*, 136 (3), 681–689.

- [32] Fatimah, I., Citradewi, P.W., Iqbal, R.M., Sheikh Mohd Ghazali, S.A.I., Yahya, A., and Purwiandono, G., 2023, Geopolymer from tin mining tailings waste using salacca leaves ash as activator for dyes and peat water adsorption, *S. Afr. J. Chem. Eng.*, 43, 257–265.
- [33] Dahliani, M.S.E., Citradewi, P.W., and Fatimah, I., 2022, Assessing adsorption capability of salacca skin waste and its biochar form for methylene blue removal from aqueous solution, *AIP Conf. Proc.*, 2645 (1), 030020.
- [34] Chan, K.T., Ong, S.T., and Ha, S.T., 2024, Adsorptive removal of Congo red dye from its aqueous solutions by tetraethylenepentamine modified peanut husks composite beads, *Desalin. Water Treat.*, 317, 100060.
- [35] Fatimah, I., Purwiandono, G., Hidayat, A., Sagadevan, S., and Kamari, A., 2022, Mechanistic insight into the adsorption and photocatalytic activity of a magnetically separable γ -Fe₂O₃/montmorillonite nanocomposite for rhodamine B removal, *Chem. Phys. Lett.*, 792, 139410.
- [36] Huang, R., Liu, Q., Huo, J., and Yang, B., 2017, Adsorption of methyl orange onto protonated cross-linked chitosan, *Arabian J. Chem.*, 10 (1), 24–32.
- [37] Langmuir, I., 1916, The constitution and fundamental properties of solids and liquids. Part I. Solids, *J. Am. Chem. Soc.*, 38 (11), 2221–2295.
- [38] Freundlich, H., 1906, Over the adsorption in solution, *J. Phys. Chem.*, 57, 385–471.
- [39] Loulidi, I., Boukhelif, F., Ouchabi, M., Amar, A., Jabri, M., Kali, A., Chraibi, S., Hadey, C., and Aziz, F., 2020, Adsorption of crystal violet onto an agricultural waste residue: Kinetics, isotherm, thermodynamics, and mechanism of adsorption, *Sci. World J.*, 2020 (1), 5873521.
- [40] Abbas, S., Javeed, T., Zafar, S., Taj, M.B., Ashraf, A.R., and Din, M.I., 2021, Adsorption of crystal violet dye by using a low-cost adsorbent – peanut husk, *Desalin. Water Treat.*, 233, 387–398.
- [41] Foroutan, R., Peighambaroust, S.J., Peighambaroust, S.H., Pateiro, M., and Lorenzo, J.M., 2021, Adsorption of crystal violet dye using activated carbon of lemon wood and activated carbon/Fe₃O₄ magnetic nanocomposite from aqueous solutions: A kinetic, equilibrium and thermodynamic study, *Molecules*, 26 (8), 2241.
- [42] Elsherif, K.M., El-Dali, A., Alkarewi, A.A., Ewlad-Ahmed, A.M., and Treban, A., 2021, Adsorption of crystal violet dye onto olive leaves powder: Equilibrium and kinetic studies, *Chem. Int.*, 7 (2), 79–89.
- [43] Ogata, F., Sugimura, K., Nagai, N., Saenjum, C., Nishiwaki, K., and Kawasaki, N., 2024, Adsorption efficiency of crystal violet from the aqueous phase onto a carbonaceous material prepared from waste cotton and polyester, *RSC Sustainability*, 2, 179–186.
- [44] Tay, C.I., and Ong, S.T., 2019, Guava leaves as adsorbent for the removal of emerging pollutant: Ciprofloxacin from aqueous solution, *J. Phys. Sci.*, 30 (2), 137–156.
- [45] Setyoprato, P., Priyantini, H.R., and Agustriyanto, R., 2019, Mass transfer kinetic model and removal capacity of acid blue 29 adsorptions onto activated carbon, *IOP Conf. Ser.: Mater. Sci. Eng.*, 703 (1), 012043.
- [46] Chan, K.T., and Ong, S.T., 2022, Optimization of methylene blue dye removal by peanut husk using Plackett-Burman design and Response Surface Methodology, *Stud. Univ. Babeş-Bolyai Chem.*, 67 (4), 121–139.
- [47] Skwierawska, A.M., Bliźniewska, M., Muza, K., Nowak, A., Nowacka, D., Zehra Syeda, S.E., Khan, M.S., and Łęska, B., 2022, Cellulose and its derivatives, coffee grounds, and cross-linked, β -cyclodextrin in the race for the highest sorption capacity of cationic dyes in accordance with the principles of sustainable development, *J. Hazard. Mater.*, 439, 129588.